PDE4 inhibition prevents preterm delivery induced by an intrauterine inflammation.

Thomas Schmitz, Evelyne Souil, Roxane Hervé, Carole Nicco, Frédéric Batteux, Guy Germain, Dominique Cabrol, Danièle Evain-Brion, Marie-Josèphe Leroy, Céline Méhats

PDE4 Inhibition Prevents Preterm Delivery Induced by an Intrauterine Inflammation

Thomas Schmitz[*, †, ‡], Evelyne Souil[§, †], Roxane Hervé[*, †], Carole Nicco[¶, †], Frédéric Batteux[¶,†], Guy Germain[‖], Dominique Cabrol[*, †, ‡], Danièle Evain-Brion[*, †], Marie-Josèphe Leroy[*, †], and Céline Méhats[*, †]

[*]Institut National de la Santé et de la Recherche Médicale, Inserm U767 F-75270 Paris cedex 06, France;

[†] Université René Descartes, Paris 5, F-75014 Paris, France;

[‡] AP-HP, Hôpital Cochin, Maternité Port-Royal, F-75014 Paris, France;

[§] Institut Cochin, Plateforme de morphologie/histologie animale, U 567, UMR 8104, F-75014 Paris, France;

[¶] Laboratoire d'Immunologie, UPRES 1833, F-75679 Paris cedex 14, France,

[‖] INRA, UMR 1198; ENVA; CNRS, FRE 2857, Biologie du Développement et Reproduction, Jouy en Josas, F-78350, France.

Running title: PDE4 inhibition blocks preterm delivery

Keywords: Reproductive immunology, cell activation, inflammation, rodent

Abstract

The aim of this study was to explore the anti-inflammatory properties of phosphodiesterases-4 (PDE4) inhibitors *in vivo* and their potential ability to prevent inflammation-induced preterm delivery. Indeed, intrauterine inflammation is the major etiology of very preterm delivery, the leading cause of neonatal mortality and morbidity. Intrauterine injection of *Escherichia Coli* LPS in 15 day pregnant mice induced an increase of PDE4 activity and PDE4B expression at the materno-fetal interface, a rise of amniotic fluid levels of TNFα, IL1β, IL6 and IL10, and provoked massive preterm delivery and fetal demise. Selective PDE4 inhibition by rolipram prevented the rise in the proinflammatory cytokines. Following the nuclear translocation of the transcription factor NFκB, as a marker of cellular activation after the inflammatory challenge, showed a time dependent sequential activation of the gestational tissues, from the uterine mesometrial to the fetal compartment, particularly in the glycogen trophoblastic cells of the placenta. This activation was disrupted by PDE4 inhibition, and inflammation-induced preterm delivery and fetal demise were prevented. PDE4 selective inhibitors may thus represent a novel effective treatment to delay inflammation-induced preterm delivery and to prevent adverse outcomes in infants.

Introduction

In industrialized countries, 5-11% of infants are born preterm, before 37 weeks of postmenstrual age (PMA). Very preterm delivery (before 32 weeks PMA) accounts for 70% of neonatal deaths and up to 75% of neonatal morbidity and contributes to long-term neurocognitive deficits and pulmonary dysfunction. Intrauterine infection has been recognized as the primary cause of very preterm delivery and favors development of periventricular leukomalacia and bronchopulmonary dysplasia (1-3). Often clinically silent, intrauterine infection triggers at the materno-fetal interface a feedforward inflammatory mechanism involving the production of cytokines, potent uterotonics and metalloproteases, which results in preterm cervical ripening, uterine contraction, and rupture of the membranes and ultimately ends by preterm delivery. Studies in Humans demonstrated higher amniotic fluid concentrations of IL-6, TNFα, and many other cytokines and chemokines in patients who subsequently delivered preterm than in patients who delivered at term (4). Systemic or intrauterine injection of IL-1β, TNFα, killed bacteria, or bacterial products induces preterm delivery in pregnant mice, rabbits, sheeps, or monkeys (5).

The cyclic nucleotides phosphodiesterases (PDE) are the enzymes that hydrolyze the ubiquitous second messengers, cAMP and cGMP, involved in the regulation of a wide variety of physiological processes including smooth muscle contractility, inflammation, and neuronal development. Eleven families of PDE are described to date with different affinities for cyclic nucleotides, specific modulators, and different patterns of expression (6). Their expression and regulation define the duration and the intensity of the signal generated by the cyclic nucleotides, building thus the specificity of the biological response.

Selective inhibitors of some PDE families are currently used in clinical practice for the

treatment of cardiovascular disorders and erectile dysfunction and other PDE inhibitors are under development for the treatment of central nervous system and inflammatory disorders. The PDE4 family is one of the major PDE family controlling inflammation. PDE4 represents the major cAMP hydrolyzing enzyme family in all immunocompetent cells. Human monocytes and neutrophils present a predominant PDE4 activity (7) and PDE4 inhibitors suppress monocytes and macrophages production of TNFα, adhesion and chemotaxis of neutrophils, as well as superoxide production and degranulation (8). The mammalian PDE4 family is encoded by four genes A, B, C, and D, composed of multiple transcriptional units and multiple promoters, which generate at least 20 different PDE4s (9). PDE4B products are thought to be specifically involved in inflammation (7, 10-12).

Herein, we investigate the ability of a PDE4 selective inhibitor, rolipram, to prevent *in vivo* preterm delivery and fetal demise in a murine model of intrauterine inflammation.

Materials and Methods

Animals

Procedures that involved mice were approved by our Institutional Committee on Animal Use and Care and were conducted in strict accordance with guidelines for the use and care of laboratory research animals promulgated by the NIH. CD-1 timed-pregnant mice were purchased from Charles River Laboratories (L'Arbresle, France). Animals were shipped on day 12 after mating and were acclimated in our facility for 3 days before use.

Mouse model of inflammation-induced preterm delivery

On day 15 of gestation (75% CD-1 gestation), a mini-laparotomy was performed under general anesthesia in the lower abdomen. Ten μg of LPS of *Escherichia coli* (O127:B8, Sigma, St Louis, MO) were injected in 100 μl PBS between the first two gestational sacs of the left uterine horn according to the technique of Elovitz *et al.* (13). Control animals received 100 μl of sterile PBS. Animals recovered in individual cages and were observed closely for any sign of morbidity (piloerection, decreased movements, vaginal bleeding). Two hours after surgery, mice received an intraperitoneal injection of 100 μl PBS containing either rolipram (3 mg/kg) or vehicle (5% DMSO). Preterm delivery was defined by delivery of at least one pup within the 48 hours following surgery. Forty-eight hours after surgery, undelivered mice were placed under general anesthesia and the number of live and dead pups in each horn was recorded. Intrauterine fetal deaths were identified by white discoloration of the pup and placenta and lack of blood flow in the umbilical cord.

Histochemistry and Immunohistochemistry

For tissue collections, mice were killed two, four or six hours after surgery. Cervical tissue and intact utero-placental units were harvested and either fixed in 10% formalin and embedded in paraffin, or snap frozen. Cervix structures were identified on 5 µm paraffin by Masson's Trichrome stain. For uterine and placenta histology and immunohistochemistry, direct adjacent sections were processed either for periodic acid-Schiff reaction (PAS), for NFκB or uterine NK (uNK) cells detection. Briefly, slides were deparaffinized through two rinses in xylene (Prolabo, Paris, France) and rehydrated through graded ethanol to phosphate-buffered saline (PBS pH 7.4) or to deionized water. To detect NFκB expression, we used the polyclonal antibody directed against the p65 form of the protein (Biosciences, Montrouge, France) diluted to 1:1,000 in PBS-BSA 1%-Triton 0.05%. To detect uNK cells, we used HRP-*Dolichos biflorus* (DBA) lectin (Sigma) diluted to 200 µg/ml in PBS-BSA 1% (14). Incubation was processed for 24h at 4^{o}C and after successives rinses, endogenous peroxidase activity was blocked with 3% hydrogen peroxide. In final, immunoreactivity was detected using the avidin-biotin Vectastain ABC Elite kit (Vector laboratories, Burlingame, CA). Color development was performed using Sigma Fast diaminobenzidine and tissue section were counterstained with Mayer's haematoxylin solution (Merck, Darmstadt, Germany). Non specific labeling by NFκB antibody was assessed on direct adjacent sections by incubation with normal rabbit serum instead of the primary antibody or by omitting the primary antibody. In both cases, immunostaining was abolished. NFκB expression and uNK cell number were analyzed by two investigators under microscope equipped with a DC 300 F camera (DMR, IM 1000) (Leica, Nussloch, Germany) using different magnifications.

Quantification of immunohistochemistry

Positively stained nuclei were counted at x200 magnification. Nuclei were counted in five distinct random fields per section, limited to the placental junctional zone and the adherent decidua basalis. The average number of positive nuclei per 1 mm^2 for each tissue sample was used for statistical analysis. All sections were counted by a single blinded investigator for internal consistency. Random sections were counted by a blinded independent investigator for external verification of the results.

Cytokines measurement in amniotic fluid

The amniotic fluids from the two gestational sacs adjacent to the site of injection were collected and snap frozen. Measurements of IL-1β, IL-6, TNFα, and IL-10 concentrations were performed using the Searchlight™ multiplex sample testing by Endogen, PerbioScience (Brebieres, France).

Progesterone measurement in dam plasma

Blood was collected by sinus orbital puncture under anesthesia, 6h after LPS instillation. Plasma samples were analyzed for progesterone concentration in duplicate by direct RIA, as previously described by Schanbacher (15) with some modifications. Charcoal-dextran solution was used instead of polyethylene glycol for the separation of bound and free radioactivity. Tritiated progesterone (1,2,6,7-^{3}H-progesterone, sp act 88 Ci/mmol) was obtained from Amersham, and a specific antiprogesterone antibody was obtained from the Pasteur Institute (Paris, France). To minimize assay variability, all plasma samples were analyzed in a single RIA. The limit of assay sensitivity was 0.1 ng/ml, and the intra-assay coefficient of variation was less than 10%.

cAMP-phosphodiesterase assay

Uterine and decidual-placental units were homogenized in ice-cold hypotonic buffer (Tris-HCl 20 mM pH 8.0, NaF 50 mM, EDTA 1 mM, EGTA 0.2 mM, Na_2PO_4 10 mM, ß-mercaptoethanol 5 mM, and a protease inhibitor cocktail: leupeptin 0.5 µg/ml, aprotinin 4 µg/ml, benzamidine 50 mM, pepstatin 0.7 µg/ml, soybean trypsin inhibitor 10 µg/ml, and PMSF 10 µg/ml added freshly before use) using an all-glass homogenizer. Aliquots of the homogenates were assayed for cAMP PDE activity according to the method of Thompson and Appleman (16). PDE activities were measured with 1 µM [^{3}H]-cAMP as a substrate. PDE4 activity was defined as the fraction of cAMP PDE activity inhibited by 10 µM rolipram. Protein concentrations were determined using the Bio-Rad protein assay (Bio-Rad Laboratories, Inc., Hercules, CA) with BSA as a standard.

Western blot analysis

Samples (30 µg protein/lane) were boiled in Laemmli buffer, subjected to electrophoresis on a 10% SDS-PAGE, and blotted onto Hybond-P transfer membrane (Amersham Pharmacia Biotech, Inc., Piscataway, NJ). Membranes were blocked in TBS-Tween 20 0.1% containing 5% nonfat milk. Polyclonal anti-PDE4B, (K118, 1:1,000, gift of M. Conti, Stanford University) were used (17). Second-step horseradish peroxidase-conjugated anti-rabbit antibodies (1:5,000) were purchased from Amersham (Amersham Pharmacia) and visualized by use of the ECL detection reagents (Amersham Pharmacia Biotech, Inc.).

Data analysis

Unless otherwise stated, significance of the difference was assessed by two-way ANOVA followed by Student's *t* test, two tailed for unpaired samples using the Prism-Graph Pad software

(GraphPad Software, San Diego, CA, USA). The difference was considered significant when $P < 0.05$.

Results

Blockade of inflammation-induced preterm delivery and reduction of fetal demise by rolipram.

Intrauterine injection of LPS provoked preterm delivery in 11 of 13 treated animals with full emptiness of the two uterine horns at 48h post-surgery. Despite maintaining pregnancies, the two remaining LPS-treated dams experienced massive *in utero* fetal deaths (75%) (Table I). However no maternal mortality or morbidity was observed. Uterine infusion of saline solution or rolipram alone resulted in minimal preterm delivery and in minimal fetal demise, only observed at the insert of the intrauterine injection. Treatment with rolipram 2h after the LPS injection blocked preterm delivery and significantly reduced fetal demise (22%).

Inhibition of inflammation-induced cervical ripening by rolipram.

Cervical ripening is characterized by a dispersion of collagen fibers of the stroma and by increase in the mucin secretion (18). To document the onset of preterm labor induced by LPS and its prevention by rolipram, sections of cervical tissue from the four groups of animals, saline- or LPS-injected with or without rolipram, were mounted and assessed for histological aspect and collagen organization with a Masson's Trichrome stain. In the LPS-injected group, 6h post-surgery, the glandular epithelium showed increased volume of the epithelial glands containing secretory vacuoles. Trichrome staining revealed loose array of disordered collagen fibers, which are histological features of compliant tissue (Figure 1B). In contrast, LPS-injected animals with rolipram exhibited characteristic of noncompliant tissue, denser, compact, heavily stain of the matrix of collagen fibers associated with undeveloped glands and absence of secretory vacuoles in the glandular epithelium as observed in the sham-operated control groups (Figure 1A, 1C, and 1D).

Decrease of inflammation-induced cytokines level rises in amniotic fluid by rolipram.

To assess that the onset of preterm labor in LPS-injected dams was concomitant to an intrauterine inflammation and that this phenomenon was prevented in the presence of rolipram, we measured the concentration of cytokines in amniotic fluids, namely TNFα, IL-1β, IL-6, and IL10, which have been reported to be involved in inflammation-induced preterm delivery (19, 20). As depicted in Figure 2, intrauterine injection of LPS induced a significant increase in the concentrations of these cytokines in the amniotic fluid, 6h post-surgery, as compared to the saline-vehicle animals, demonstrating that an intrauterine inflammation has been mounted against LPS in these animals. The injection of rolipram alone did not significantly affect the concentrations of these factors; but it significantly diminished the increase of TNFα, IL-1β, and IL-6 concentration in the amniotic fluids of LPS-injected animals while not significantly affecting IL-10 concentration.

No change in progesterone plasma levels during intrauterine inflammation.

In the same mice, the concentration of circulating progesterone was evaluated 6h post-surgery. Mice of each group demonstrated high plasma progesterone levels without significant difference between the four groups (Figure 3).

Expression of PDE4B2 in decidual and placental units

To investigate the level of PDE4 activity in mouse gestational tissues at the time of the injection of rolipram, we measured PDE activity in whole homogenates of uterine tissues (myometrium and endometrium) or placental units, with the decidual cap still attached, collected 2h after surgery. As reported in Figure 4, PDE4 activity, gauged as rolipram-sensitive activity, represented almost half of total cAMP-PDE activity in both tissues. Uterine tissues contained 10-

times more cAMP-PDE and PDE4 activities than decidual-placental units, however no change was observed upon stimulation by LPS. Meanwhile, PDE4 activity increased significantly in the decidua-placental unit. Western blot analysis of PDE4B expression in the decidua-placental unit showed an increase in the signal of a short product of PDE4B gene at 72 kDa, corresponding to the PDE4B2 form. PDE4B2 was also expressed in uterine tissues, but no change upon LPS challenge was observed (Figure 4).

Inhibition of LPS-induced NFκB nuclear translocation in the gestational tissues by rolipram

LPS promotes nuclear translocation and activation of the transcriptional factor, NFκB, most often found as a p50-p65 dimer unit. The p65 subunit is mainly responsible of the nuclear translocation of this complex, a nuclear localization signal being coded within its protein sequence (21). Thus, we looked for the cellular localization of p65-NFκB subunit in gestational tissues using immunohistochemistry 2, 4, and 6h after surgery (Figure 5). In uterine tissues, p65-NFκB was readily in the nucleus of endometrial cells in sham-operated animals at H0 and remained in the nucleus at 2, 4, and 6h, while rare cytoplasmic signals were detected in the myometrium and were not affected by LPS treatment (data not shown). p65-NFκB was found rarely within the nucleus of cells of the decidua-placental units in sham-operated animals at 2 (Figure 5B), 4, and 6h. Markedly, a significantly high number of stained nuclei was observed at 2h in the maternal cells in the decidual cap of LPS-treated animals (Figure 5C). This number of stained nuclei remained high at 4h in the maternal compartment and was then also observed in the fetal cells of the placenta. At 6h, only glycogen trophoblasts, recognized by their characteristic histological aspect and their staining with PAS (22) (Figure 5A), depicted a nuclear signal in LPS-treated animals (Figure 5D). Treatment with rolipram abolished the nuclear signals in both maternal and fetal compartments (Figure 5E). Quantitative analysis of nuclear NFκB

staining demonstrated significant inhibition of nuclear NFκB translocation by rolipram 4 and 6h after surgery (Figure 6).

Inhibition of inflammation-induced mesometrial uNK recruitment by rolipram

Because uNK cells are the main inflammatory cells within gestational tissues, we checked their presence in the decidual cap upon treatment using the highly selective DBA lectin. An increase in the number of uNK cells in the mesometrial compartment (Figure 7) 4 hours after LPS treatment was observed. This increase was completely prevented in the presence of rolipram. However the NFκB nuclear signal and uNK cells were not superposed.

Discussion

In the present study, we report for the first time that PDE4 inhibition blocks intrauterine inflammation *in vivo* and prevents preterm delivery and fetal demise in a mouse model. We provide evidence that intrauterine inflammation evolves from the maternal to the fetal compartment. Moreover, our data point out an unrecognized role for the glycogen trophoblasts in these processes.

Murine models of preterm delivery have been developed these last decades, based on systemic or local injection of heated-dead bacteria or bacterial products, including LPS at doses ranging from 10 µg to 250 µg, to provide new insights into the molecular events underlying causes of preterm labor (reviewed in (5, 21)). Indeed, in Humans, the ethical status of the fetus and large discrepancies in clinical variables among patients at the time of asserted preterm labor prohibit any possibility to conduct experimentally controlled basic research. The murine preterm labor model provides a powerful mean for maintaining tight experimental controls in an *in vivo* context. Using such model we showed that an injection of a low dose of LPS in the uterus between two gestational sacs caused 85% of preterm delivery with full emptiness of the uterus and 75% of fetal demise in the undelivered dams within 48h. PDE4 inhibition two hours after the intrauterine inflammatory challenge blocks preterm labor as documented by the absence of morphologic changes in the cervix and subsequent preterm delivery. Furthermore PDE4 inhibition diminished to more than the third the rate of fetal demise in undelivered dams (22% *vs.* 75%), though this figure underestimates the rate of intrauterine death before expulsion in the LPS-injected group.

We also showed increase in the amniotic fluid concentration of key cytokines 6h after the inflammatory challenge, namely, TNFα, IL-1β, IL-6, and IL-10. Elevated levels of TNFα, IL-1β, and IL-6 are found in amniotic fluid during pregnancies complicated by infection and preterm

delivery in Humans (24). IL-6 level has been proposed as a marker for the prediction of preterm delivery (25). TNFα, IL-1β and IL-6 can induce the production of both prostaglandins and metalloproteases leading to preterm delivery (19, 20). Double knock-outs for TNFα and IL-1β receptors are refractory to bacterially induced preterm labor (22). Conversely, the anti-inflammatory cytokine IL-10 has been shown to prolong gestation and to diminish fetal demise in bacterially treated dams when administrated alone or in combination with antibiotics (23). In our model, PDE4 inhibition blocked rise in TNFα, IL-1β, and IL-6, while had no significant effect on IL-10 level. Manipulation of these cytokines by PDE4 inhibition may provide a mechanism by which rolipram prevents both inflammation-induced delivery and fetal demise.

Several compounds have been shown to delay inflammation-induced preterm delivery, lactoferrin, betamethasone, pharmacologic doses of progesterone, or a progestin derivative, medroxyprogesterone acetate, antioxidant N-acetylcysteine, platelet-activating factor antagonist, metalloprotease inhibitor phosphoramidon, PGHS inhibitors such as indomethacin, PGHS-1 and PGHS-2 inhibitors, $PGF_{2\alpha}$ receptor antagonist (13, 24-30). Each of these compounds interacts with one or more of the factors believed to have a role in the inflammatory cascade leading to preterm birth. However, in all these studies, most of the undelivered fetus died *in utero,* the rate of fetal demises ranging to 60-100%, although the drugs were given before the inflammatory challenge, in the contrary to the present study where PDE4 inhibition starts 2h after LPS challenge.

One major discrepancy between humans and mice gestation consists on the fact that maintenance of gestation in mice depends on the production of progesterone by the corpus luteum all along the gestation (31). However, despite the fact that physiological progesterone supplementation prolongs the interval to delivery in ovariectomized animals, it has no effect in bacterially exposed animals, implying that progesterone withdrawal is not the priming event of

inflammation-induced preterm delivery . Consistent with others studies, we documented no significant decrease in plasmatic progesterone concentration following intrauterine inflammatory challenge at a time when labor has started with cervical modification (13, 32).

PDE4 inhibition impacts both uterine and decidua-placental tissues, insofar as we detected PDE4 activity in these tissues. We documented that PDE4B2, a PDE4 isoform involved in inflammation, is induced in the decidual-placental unit by LPS, concomitantly to a significant increase in PDE4 activity. These data suggest a role for PDE4B2 in this compartment upon LPS inflammatory cascade, while no change of PDE4 activity or PDE4B2 expression was observed in the uterine tissues.

To identify, within the materno-fetal interface, the cells involved in the LPS inflammatory cascade, we searched by immunohistochemistry the localization of NFκB. In our model, we observed a sequential nuclear translocation of NFκB from the maternal to the fetal compartment. We evidenced nuclear localization of NFκB 2h after the inflammatory challenge in the uterine mesometrial compartment (33).We also confirmed an increase of the number of uNK cells after the LPS challenge, consistent with earlier report (34). As PDE4B2 expression is reported high in immunocompetent cells (35), increase of the number of uNK cells may then account for the increased presence of PDE4B2 within the decidual-placental unit. The presence of active uNK cells has been shown to be controlled by IL-10 (34). The IL-10 knock-out strain displays high uNK cell number in the uterine mesometrial compartment. Moreover this KO strain is highly sensitive to very low doses of LPS, which induce massive fetal demise, not seen in the wild-type littermates. It has been speculates that uNK cells may serve as a fail-safe mechanism to terminate pregnancy, when excessive inflammatory or other insults are experienced (34).

Four hours after the LPS insult, NFκ B was also localized in the nucleus of a specific trophoblast in the fetal compartment, the glycogen trophoblast. In mice, glycogen trophoblasts

appear in the junctional zone of the placenta at 12d and invade the uterine mesometrial compartment until term (36, 37). Their functions remain largely unknown; however absence of differentiation of these cells in IGF-2 KO strain delays the onset of term labor (38). Further studies on these specialized cells are required to decipher their role in nourishing the feedforward mechanisms of intrauterine inflammation to preterm delivery.

Interestingly, we showed that the nuclear translocation of NFκB is prevented by PDE4 inhibition in the cells of the materno-fetal interface, with no more nuclear signal six hours after LPS challenge. In a LPS-induced uveitis model in rat, p65-NFκB was also excluded of the nucleus of iris-ciliary body of LPS-treated animals by rolipram (39). Therefore, prevention of nuclear NFκB translocation may represent a hitherto unnoticed molecular mechanism by which rolipram or PDE4 inhibition exerts its antiinflammatory effect.

The therapeutic strategy in case of preterm labor, namely tocolysis, is aimed to delay birth by inhibiting uterine contractions (40). However, conventional methods of tocolysis are ineffective on the inflammation component of preterm labor and expose longer the fetus to stimuli noxious for the immature brain. Novel tocolytic agents that down-regulate intrauterine inflammation may then offer a solution for the prolongation of pregnancy, safe for the fetus. We showed previously in Humans that PDE4 inhibition blocks spontaneous contractions of myometrial strips. It also abolished the activation in fetal membranes of metalloproteases and prostaglandin syntheses that may lead to preterm premature rupture of the membranes (41-43). Here, we report that PDE4 inhibition blocks intrauterine inflammation, which may injure the fetus if uncontrolled. PDE4 inhibitors may thus represent a novel class of tocolytic, also able to control inflammation and its consequences for the infant.

Acknowledgements

We are indebted to the Dr. Michelle Breuillet-Fouché for helpful discussions, Dr. André Malassiné for his expertise on placental development, and Pr. Marco Conti for the PDE4B specific antibodies.

References

1. Goldenberg, R. L., J. C. Hauth, and W. W. Andrews. 2000. Intrauterine infection and preterm delivery. *N. Engl. J. Med.* 342:1500-1507.
2. Slattery, M. M., and J. J. Morrison. 2002. Preterm delivery. *Lancet.* 360:1489-1497.
3. Yoon, B. H., C. W. Park, and T. Chaiworapongsa. 2003. Intrauterine infection and the development of cerebral palsy. *Bjog.* 110 Suppl 20:124-127.
4. Romero, R., H. Munoz, R. Gomez, D. M. Sherer, F. Ghezzi, A. Ghidini, O. Alfi, G. DeVore, and L. Randolph. 1995. Two thirds of spontaneous abortion/fetal deaths after genetic midtrimester amniocentesis are the result of a pre-existing subclinical inflammatory process of the amniotic cavity. *Am. J. Obstet. Gynecol.* 172:261.
5. Elovitz, M. A., and C. Mrinalini. 2004. Animal models of preterm birth. *Trends Endocrinol. Metab.* 15:479-487.
6. Mehats, C., C. B. Andersen, M. Filopanti, S. L. Jin, and M. Conti. 2002. Cyclic nucleotide phosphodiesterases and their role in endocrine cell signaling. *Trends Endocrinol. Metab.* 13:29-35.
7. Wang, P., P. Wu, K. M. Ohleth, R. W. Egan, and M. M. Billah. 1999. Phosphodiesterase 4B2 is the predominant phosphodiesterase species and undergoes differential regulation of gene expression in human monocytes and neutrophils. *Mol. Pharmacol.* 56:170-174.
8. Houslay, M. D. 2001. PDE4 cAMP-specific phosphodiesterases. *Prog. Nucl. Acid Res. Mol. Biol.* 69:249-315.
9. Conti, M., W. Richter, C. Mehats, G. Livera, J. Y. Park, and C. Jin. 2003. Cyclic AMP-specific PDE4 phosphodiesterases as critical components of cyclic AMP signaling. *J. Biol. Chem.* 278:5493-5496.
10. Ariga, M., B. Neitzert, S. Nakae, G. Mottin, C. Bertrand, M. P. Pruniaux, S. L. Jin, and

M. Conti. 2004. Nonredundant function of phosphodiesterases 4D and 4B in neutrophil recruitment to the site of inflammation. *J. Immunol.* 173:7531-7538.

11. Jin, S. L., L. Lan, M. Zoudilova, and M. Conti. 2005. Specific role of phosphodiesterase 4B in lipopolysaccharide-induced signaling in mouse macrophages. *J. Immunol.* 175:1523-1531.

12. Ma, D., P. Wu, R. W. Egan, M. M. Billah, and P. Wang. 1999. Phosphodiesterase 4B gene transcription is activated by lipopolysaccharide and inhibited by interleukin-10 in human monocytes. *Mol. Pharmacol.* 55:50-57.

13. Elovitz, M. A., Z. Wang, E. K. Chien, D. F. Rychlik, and M. Phillippe. 2003. A new model for inflammation-induced preterm birth: the role of platelet-activating factor and Toll-like receptor-4. *Am. J. Pathol.* 163:2103-2111.

14. Paffaro, V. A., Jr., M. C. Bizinotto, P. P. Joazeiro, and A. T. Yamada. 2003. Subset classification of mouse uterine natural killer cells by DBA lectin reactivity. *Placenta.* 24:479-488.

15. Schanbacher, B. D. 1979. Radioimmunoassay of ovine and bovine serum progesterone without extraction and chromatography. *Endocr. Res. Commun.* 6:265-277.

16. Thompson, W. J., G. Brooker, and M. M. Appleman. 1974. Assay of cyclic nucleotide phosphodiesterases with radioactive substrates. *Methods Enzymol.* 38:205-212.

17. Iona, S., M. Cuomo, T. Bushnik, F. Naro, C. Sette, M. Hess, E. R. Shelton, and M. Conti. 1998. Characterization of the rolipram-sensitive, cyclic AMP-specific phosphodiesterases: identification and differential expression of immunologically distinct forms in the rat brain. *Mol. Pharmacol.* 53:23-32.

18. Leppert, P. C. 1995. Anatomy and physiology of cervical ripening. *Clin. Obstet. Gynecol.* 38:267-279.

19. Baggia, S., M. G. Gravett, S. S. Witkin, G. J. Haluska, and M. J. Novy. 1996. Interleukin-1 beta intra-amniotic infusion induces tumor necrosis factor-alpha, prostaglandin production, and preterm contractions in pregnant rhesus monkeys. *J. Soc. Gynecol. Investig.* 3:121-126.

20. Brown, N. L., S. A. Alvi, M. G. Elder, P. R. Bennett, and M. H. Sullivan. 1998. Interleukin-1beta and bacterial endotoxin change the metabolism of prostaglandins E2 and F2alpha in intact term fetal membranes. *Placenta.* 19:625-630.

21. Hirsch, E., and H. Wang. 2005. The molecular pathophysiology of bacterially induced preterm labor: insights from the murine model. *J. Soc. Gynecol. Investig.* 12:145-155.

22. Hirsch, E., Y. Filipovich, and M. Mahendroo. 2006. Signaling via the type I IL-1 and TNF receptors is necessary for bacterially induced preterm labor in a murine model. *Am. J. Obstet. Gynecol.* 194:1334-1340.

23. Terrone, D. A., B. K. Rinehart, J. P. Granger, P. S. Barrilleaux, J. N. Martin, Jr., and W. A. Bennett. 2001. Interleukin-10 administration and bacterial endotoxin-induced preterm birth in a rat model. *Obstet. Gynecol.* 98:476-480.

24. Buhimschi, I. A., C. S. Buhimschi, and C. P. Weiner. 2003. Protective effect of N-acetylcysteine against fetal death and preterm labor induced by maternal inflammation. *Am. J. Obstet. Gynecol.* 188:203-208.

25. Gross, G., T. Imamura, S. K. Vogt, D. F. Wozniak, D. M. Nelson, Y. Sadovsky, and L. J. Muglia. 2000. Inhibition of cyclooxygenase-2 prevents inflammation-mediated preterm labor in the mouse. *Am. J. Physiol. Regul. Integr. Comp. Physiol.* 278:R1415-1423.

26. Kaga, N., Y. Katsuki, M. Obata, and Y. Shibutani. 1996. Repeated administration of low-dose lipopolysaccharide induces preterm delivery in mice: a model for human preterm parturition and for assessment of the therapeutic ability of drugs against preterm delivery.

Am. J. Obstet. Gynecol. 174:754-759.

27. Koscica, K. L., G. Sylvestre, and S. E. Reznik. 2004. The effect of phosphoramidon on inflammation-mediated preterm delivery in a mouse model. *Am. J. Obstet. Gynecol.* 190:528-531.

28. Loftin, C. D., D. B. Trivedi, and R. Langenbach. 2002. Cyclooxygenase-1-selective inhibition prolongs gestation in mice without adverse effects on the ductus arteriosus. *J. Clin. Invest.* 110:549-557.

29. Peri, K. G., C. Quiniou, X. Hou, D. Abran, D. R. Varma, W. D. Lubell, and S. Chemtob. 2002. THG113: a novel selective FP antagonist that delays preterm labor. *Semin. Perinatol.* 26:389-397.

30. Sakai, M., K. Tanebe, Y. Sasaki, K. Momma, S. Yoneda, and S. Saito. 2001. Evaluation of the tocolytic effect of a selective cyclooxygenase-2 inhibitor in a mouse model of lipopolysaccharide-induced preterm delivery. *Mol. Hum. Reprod.* 7:595-602.

31. Malassine, A., J. L. Frendo, and D. Evain-Brion. 2003. A comparison of placental development and endocrine functions between the human and mouse model. *Hum. Reprod. Update.* 9:531-539.

32. Hirsch, E., and R. Muhle. 2002. Intrauterine bacterial inoculation induces labor in the mouse by mechanisms other than progesterone withdrawal. *Biol. Reprod.* 67:1337-1341.

33. Croy, B. A., A. A. Ashkar, R. A. Foster, J. P. DiSanto, J. Magram, D. Carson, S. J. Gendler, M. J. Grusby, N. Wagner, W. Muller, and M. J. Guimond. 1997. Histological studies of gene-ablated mice support important functional roles for natural killer cells in the uterus during pregnancy. *J. Reprod. Immunol.* 35:111-133.

34. Murphy, S. P., L. D. Fast, N. N. Hanna, and S. Sharma. 2005. Uterine NK cells mediate inflammation-induced fetal demise in IL-10-null mice. *J. Immunol.* 175:4084-4090.

35. Houslay, M. D., P. Schafer, and K. Y. Zhang. 2005. Keynote review: phosphodiesterase-4 as a therapeutic target. *Drug. Discov. Today.* 10:1503-1519.

36. Adamson, S. L., Y. Lu, K. J. Whiteley, D. Holmyard, M. Hemberger, C. Pfarrer, and J. C. Cross. 2002. Interactions between trophoblast cells and the maternal and fetal circulation in the mouse placenta. *Dev. Biol.* 250:358-373.

37. Coan, P. M., A. C. Ferguson-Smith, and G. J. Burton. 2005. Ultrastructural changes in the interhaemal membrane and junctional zone of the murine chorioallantoic placenta across gestation. *J. Anat.* 207:783-796.

38. Lopez, M. F., P. Dikkes, D. Zurakowski, and L. Villa-Komaroff. 1996. Insulin-like growth factor II affects the appearance and glycogen content of glycogen cells in the murine placenta. *Endocrinology.* 137:2100-2108.

39. Chi, Z. L., S. Hayasaka, X. Y. Zhang, Y. Hayasaka, and H. S. Cui. 2004. Effects of rolipram, a selective inhibitor of type 4 phosphodiesterase, on lipopolysaccharide-induced uveitis in rats. *Invest Ophthalmol. Vis. Sci.* 45:2497-2502.

40. Keirse, M. J. 2003. The history of tocolysis. *Bjog.* 110 Suppl 20:94-97.

41. Leroy, M. J., I. Cedrin, M. Breuiller, Y. Giovagrandi, and F. Ferre. 1989. Correlation between selective inhibition of the cyclic nucleotide phosphodiesterases and the contractile activity in human pregnant myometrium near term. *Biochem. Pharmacol.* 38:9-15.

42. Mehats, C., G. Tanguy, B. Paris, B. Robert, N. Pernin, F. Ferre, and M. J. Leroy. 2000. Pregnancy induces a modulation of the cAMP phosphodiesterase 4- conformers ratio in human myometrium: consequences for the utero- relaxant effect of PDE4-selective inhibitors. *J. Pharmacol. Exp. Ther.* 292:817-823.

43. Oger, S., C. Mehats, E. Dallot, D. Cabrol, and M. J. Leroy. 2005. Evidence for a role of

phosphodiesterase 4 in lipopolysaccharide-stimulated prostaglandin E2 production and matrix metalloproteinase-9 activity in human amniochorionic membranes. *J. Immunol.* 174:8082-8089.

Footnotes

1 This work was supported by the March of Dimes Birth Defects Foundation Grant n°6-FY03-6

2 Abbreviations used

PDE, phosphodiesterase; PMA, postmenstrual age; uNK, uterine Natural Killer; DBA, Dolichos biflorus; PAS, Periodic acid Schiff

3 Corresponding author and reprint request:

Céline Méhats

INSERM, U767, Faculté de Pharmacie

4 Avenue de l'Observatoire

75270 Paris cedex 06, FRANCE

Tel: 33 1 44 07 39 91 Fax: 33 1 44 07 39 92

Email: mehats@cochin.inserm.fr

Figure Legends

Figure 1-Inhibition of inflammation-induced cervical ripening by rolipram. Cervical sections were assessed, 6h after the inflammatory challenge, for histological aspect and collagen content (blue-green coloration) using Masson's trichrome stain. (A) saline-vehicle, (B) LPS-vehicle, (C) saline-rolipram, and (D) LPS-rolipram treated animals. Representative sections of the tissues obtained from five animals per group are shown. Scale bar = 400 µm

Figure 2-Inhibition of inflammation-induced cytokines synthesis in amniotic fluid by rolipram. Concentrations of TNFα, Il-1β, Il-6, and IL-10 were measured by multiplex ELISA in amniotic fluid of saline-vehicle, saline-rolipram, LPS-vehicle, and LPS-rolipram dams, 6h after LPS challenge. Box-and-whisker representations indicate the median and the overall range of distribution of the measurements, the bars indicating the smallest and greatest values, obtained from 12 different animals. Significant difference from saline-vehicle group: *, $P<0.05$; **, $P<0.01$.

Figure 3-Progesterone plasma level during intrauterine inflammation. Concentration of progesterone was measured by RIA in plasma of saline-vehicle, saline-rolipram, LPS-vehicle, and LPS-rolipram dams, 6h after LPS challenge. Box-and-whisker representations indicate the median and the overall range of distribution of the measurements, the bars indicating the smallest and greatest values, obtained from 12 different animals.

Figure 4-Expression of PDE4B2 in decidual and placental units. (A) Uterine tissues and decidual-placental unit from saline-vehicle, LPS-vehicle dams, 2h after LPS challenge, were homogenized and cAMP PDE activity was measured in the absence or the presence of 10 µM rolipram. Data

are expressed as the mean ± SEM for three different experiments using a total of five animals per group. *, P<0.05: significantly different from saline-vehicle group. (B) Decidual-placental units from saline-vehicle or LPS-vehicle dams for the indicated time were homogenized. Thirty micrograms of the protein extracts were subjected to 8% SDS-PAGE and electroblotted. PDE4B protein was detected by incubation with the polyclonal antibodies K118 and a peroxydase-conjugated secondary antibody. Representative blots of three different experiments performed with tissues from three different animals are shown.

Figure 5-Nuclear localization of NFκB in decidual and placental units during intrauterine inflammation. Diagram representing decidual-placental units on 15th gestational days. The square represents the regions photographied in the mesometrial side (M), Junctional zone (JZ) and Labyrinthe (L). (A) PAS staining of a saline-vehicle dam. (B) and (C) NFkB immunostaining in saline-vehicle and LPS-vehicle dams, respectively, 2h after the surgery. (D) and (E) NFkB immunostaining in LPS-vehicle and LPS-rolipram dams, respectively, 6h after the surgery. Arrowheads indicate glycogen trophoblasts in the junctional zone. Representative sections obtained from six different animals per group are shown. Scale bar = 100 μm.

Figure 6-Prevention of sustained NFκB nuclear location by rolipram. Positively NFκB nuclei were counted in the decidual-placental unit sections obtained from saline-vehicle, LPS-vehicle, saline-rolipram, and LPS-rolipram dams, for the indicated time after LPS challenge. Data are expressed as the mean ± SEM obtained from six animals per group. **, P<0.01: significantly different from saline-vehicle group.

Figure 7-Prevention of uNK cell number increase in gestational tissues by rolipram. Decidual-placental units were assessed, 4h after the inflammatory challenge, for uNKcells presence using the DBA lectin (A) saline-vehicle, (B) LPS-vehicle, (C) saline-rolipram, and (D) LPS-rolipram treated animals. Representative sections of the tissues obtained from five animals per group are shown. Scale bar = 100 μm.

Table I: Prevention of LPS-preterm delivery and fetal demise by rolipram

Treatment group	n	Preterm delivery	Live pups/ undelivered dam (n)	Dead pups/ undelivered dam (n)
saline / vehicle	12	1	8.7 ± 1.1 (11)	0.7 ± 0.3 (11)
LPS / vehicle	13	11***	2.5 ± 2.5 (2)	7.5 ± 1.5 (2)
saline / rolipram	11	1	10.2 ± 1.5 (10)	0.9 ± 0.5 (10)
LPS / rolipram	13	2	7.4 ± 1.2 (11)	2.1 ± 0.6* (11)

The Fisher exact test was applied for comparison of preterm delivery rate in each group. *** P<0.001 versus saline- vehicle group. For comparison of the number of live and dead pups per undelivered dam, expressed as mean ± SEM, statistical difference between groups was assessed by two-way ANOVA, followed by Student's *t* test, two tailed for unpaired samples. * P<0.05, versus the saline-vehicle group.

Schmitz et al. Figure 1

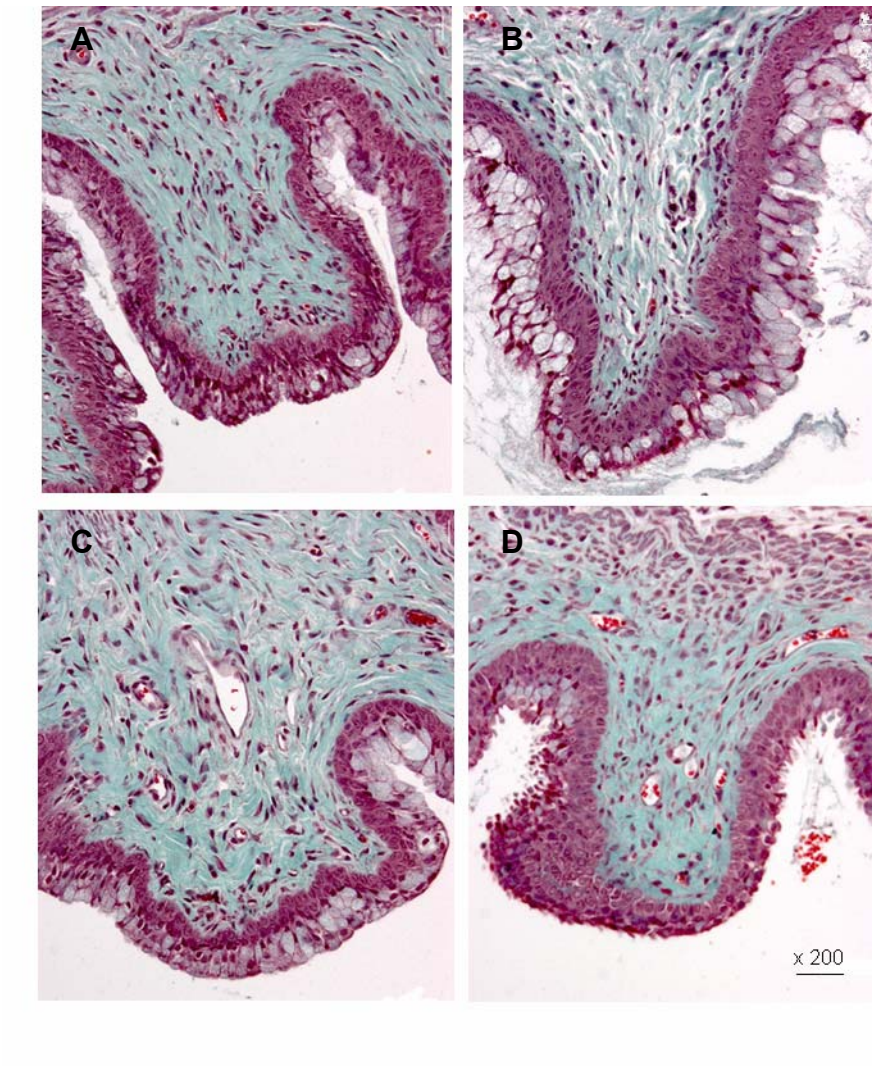

Schmitz et al. Figure 2

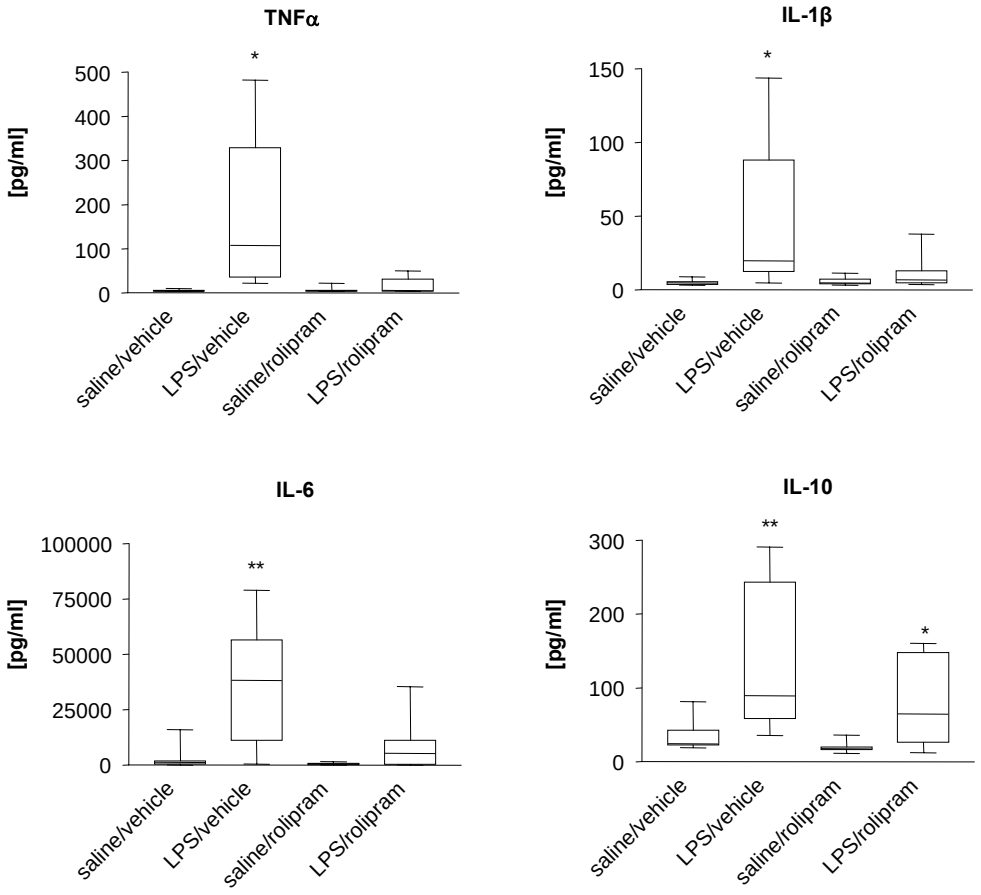

Schmitz et al. Figure 3

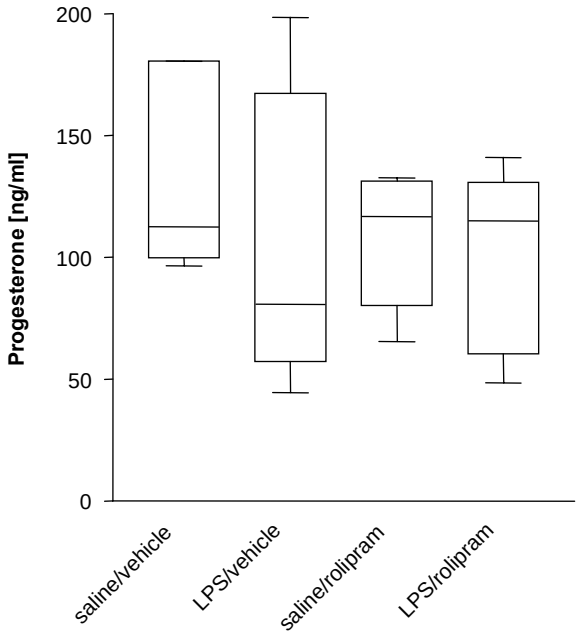

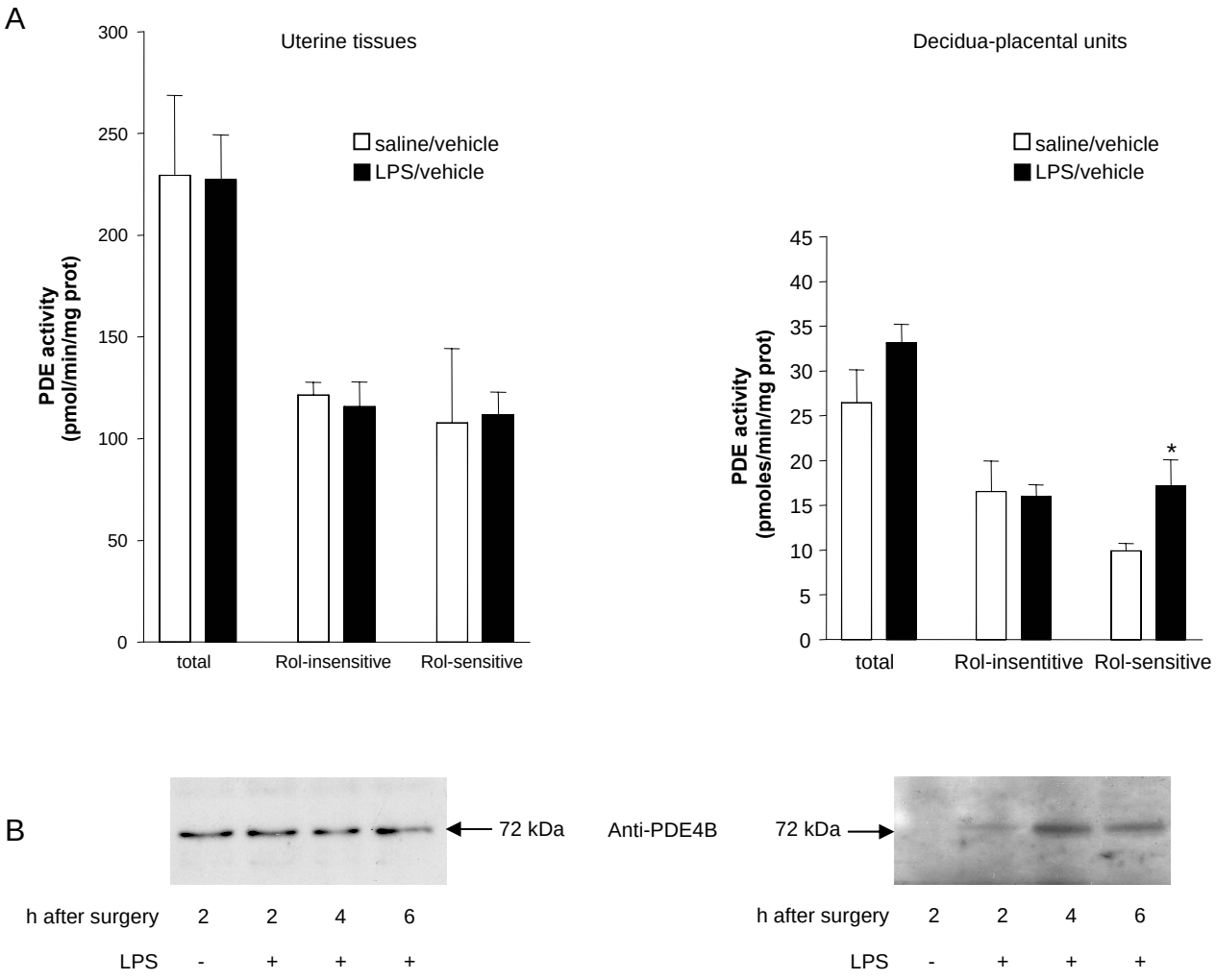

Schmitz et al. Figure 5

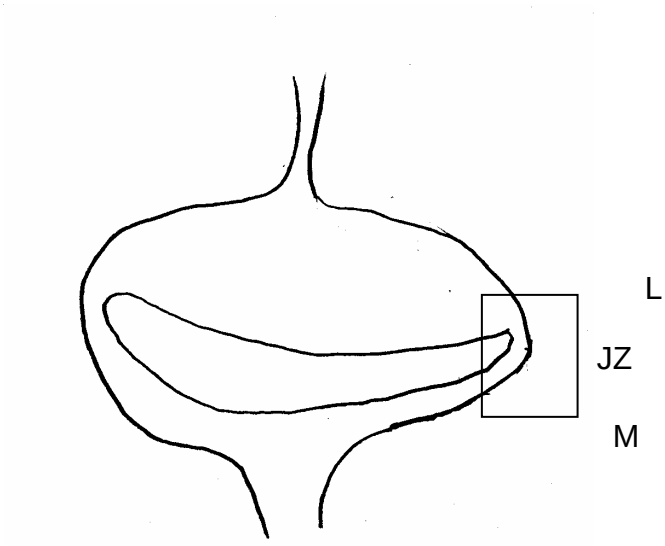

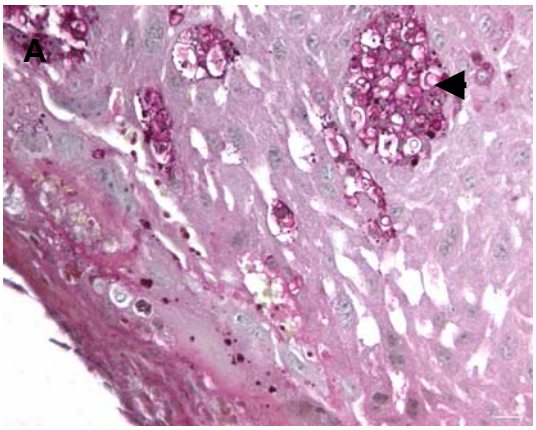

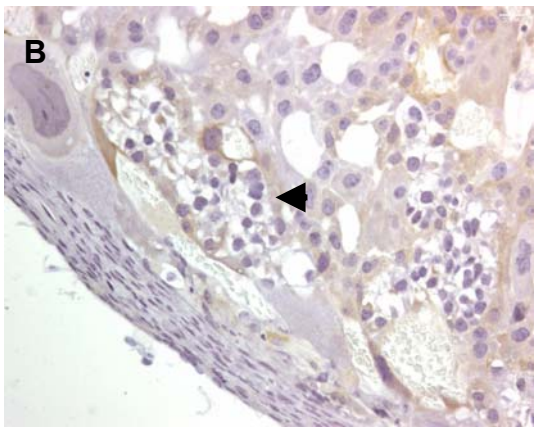

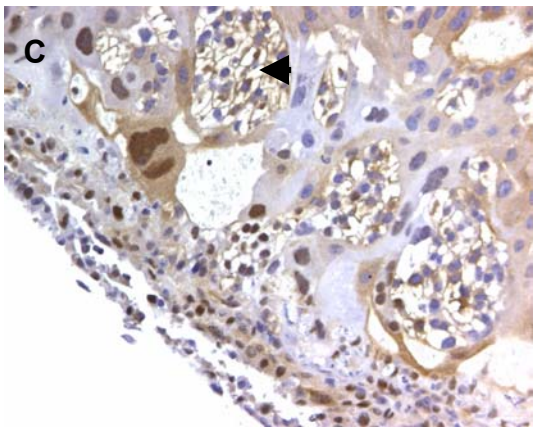

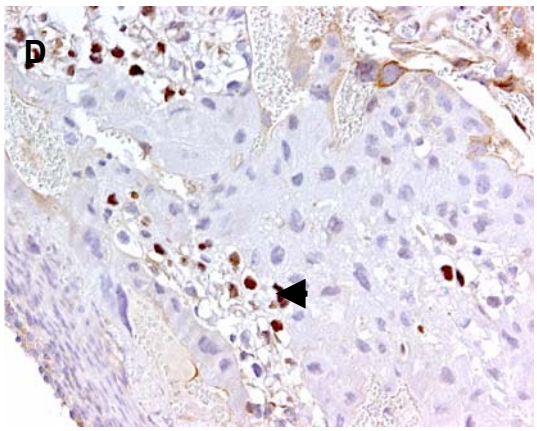

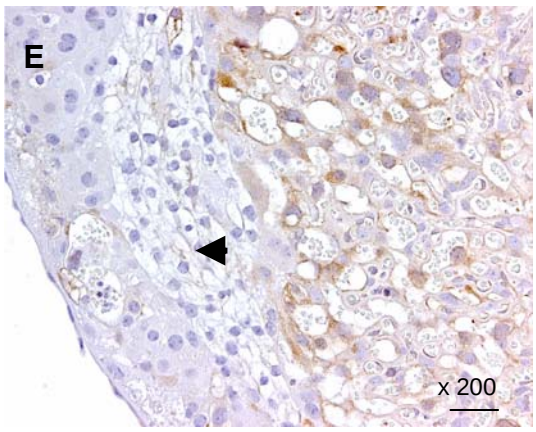

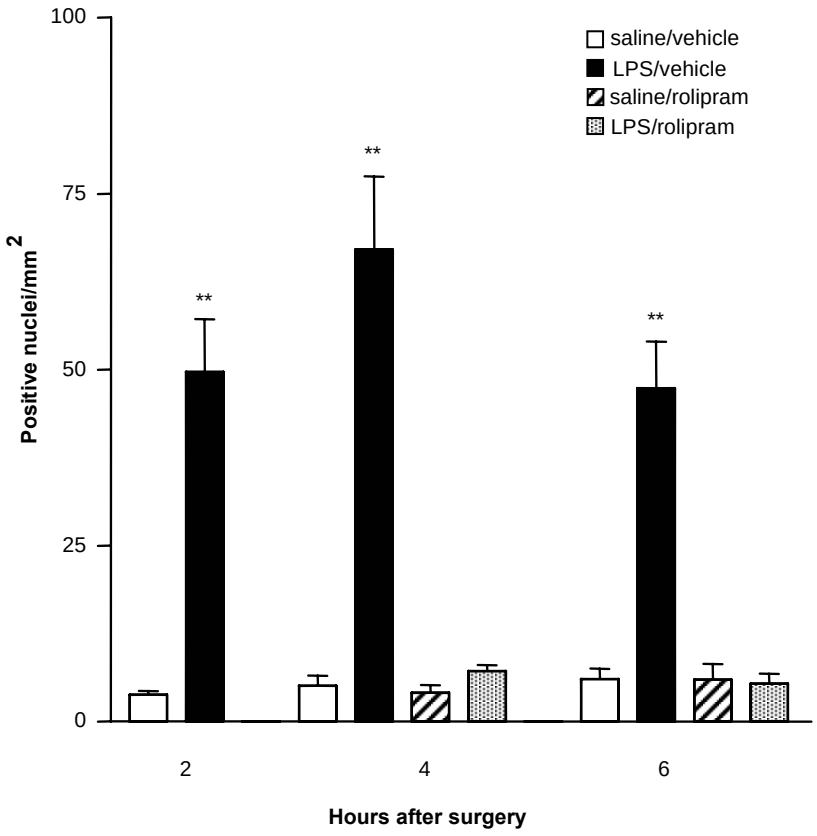

Schmitz et al. Figure 7